Gamma-Ray Emission from the Shell of Supernova Remnant W44 Revealed by the Fermi LAT

A. A. Abdo, *et al.*

Science **327**, 1103 (2010);
DOI: 10.1126/science.1182787

Gamma-Ray Emission from the Shell of Supernova Remnant W44 Revealed by the Fermi LAT

A. A. Abdo,[1]* M. Ackermann,[2] M. Ajello,[2] L. Baldini,[3] J. Ballet,[4] G. Barbiellini,[5,6] M. G. Baring,[7] D. Bastieri,[8,9] B. M. Baughman,[10] K. Bechtol,[2] R. Bellazzini,[3] B. Berenji,[2] R. D. Blandford,[2] E. D. Bloom,[2] E. Bonamente,[11,12] A. W. Borgland,[2] J. Bregeon,[3] A. Brez,[3] M. Brigida,[13,14] P. Bruel,[15] T. H. Burnett,[16] S. Buson,[9] G. A. Caliandro,[13,14] R. A. Cameron,[2] P. A. Caraveo,[17] J. M. Casandjian,[4] C. Cecchi,[11,12] Ö. Çelik,[18,19,20] A. Chekhtman,[1,21] C. C. Cheung,[18] J. Chiang,[2] S. Ciprini,[11,12] R. Claus,[2] I. Cognard,[22] J. Cohen-Tanugi,[23] L. R. Cominsky,[24] J. Conrad,[25,26]† S. Cutini,[27] C. D. Dermer,[1] A. de Angelis,[28] F. de Palma,[13,14] S. W. Digel,[2] E. do Couto e Silva,[2] P. S. Drell,[2] R. Dubois,[2] D. Dumora,[29,30] C. Espinoza,[31] C. Farnier,[23] C. Favuzzi,[13,14] S. J. Fegan,[15] W. B. Focke,[2] P. Fortin,[15] M. Frailis,[28] Y. Fukazawa,[32] S. Funk,[2] P. Fusco,[13,14] F. Gargano,[14] D. Gasparrini,[27] N. Gehrels,[18,33] S. Germani,[11,12] G. Giavitto,[34] B. Giebels,[15] N. Giglietto,[13,14] F. Giordano,[13,14] T. Glanzman,[2] G. Godfrey,[2] I. A. Grenier,[4] M.-H. Grondin,[29,30] J. E. Grove,[1] L. Guillemot,[29,30] S. Guiriec,[35] Y. Hanabata,[32] A. K. Harding,[18] M. Hayashida,[2] E. Hays,[18] R. E. Hughes,[10] M. S. Jackson,[25,26,36] G. Jóhannesson,[2] A. S. Johnson,[2] T. J. Johnson,[18,33] W. N. Johnson,[1] T. Kamae,[2] H. Katagiri,[32] J. Kataoka,[37,38] J. Katsuta,[39,40] N. Kawai,[37,41] M. Kerr,[16] J. Knödlseder,[42] M. L. Kocian,[2] M. Kramer,[31,43] M. Kuss,[3] J. Lande,[2] L. Latronico,[3] M. Lemoine-Goumard,[29,30] F. Longo,[5,6] F. Loparco,[13,14] B. Lott,[29,30] M. N. Lovellette,[1] P. Lubrano,[11,12] A. G. Lyne,[31] G. M. Madejski,[2] A. Makeev,[1,21] M. N. Mazziotta,[14] J. E. McEnery,[18] C. Meurer,[24,25] P. F. Michelson,[2] W. Mitthumsiri,[2] T. Mizuno,[32] C. Monte,[13,14] M. E. Monzani,[2] A. Morselli,[44] I. V. Moskalenko,[2] S. Murgia,[2] T. Nakamori,[37] P. L. Nolan,[2] J. P. Norris,[45] A. Noutsos,[31] E. Nuss,[23] T. Ohsugi,[32] N. Omodei,[3] E. Orlando,[46] J. F. Ormes,[45] D. Paneque,[2] D. Parent,[29,30] V. Pelassa,[23] M. Pepe,[11,12] M. Pesce-Rollins,[3] F. Piron,[23] T. A. Porter,[47] S. Rainò,[13,14] R. Rando,[8,9] M. Razzano,[3] A. Reimer,[48,2] O. Reimer,[48,2] T. Reposeur,[29,30] L. S. Rochester,[2] A. Y. Rodriguez,[49] R. W. Romani,[2] M. Roth,[16] F. Ryde,[36,26] H. F.-W. Sadrozinski,[47] D. Sanchez,[15] A. Sander,[10] P. M. Saz Parkinson,[47] J. D. Scargle,[50] C. Sgrò,[3] E. J. Siskind,[51] D. A. Smith,[29,30] P. D. Smith,[10] G. Spandre,[3] P. Spinelli,[13,14] B. W. Stappers,[31] F. W. Stecker,[18] M. S. Strickman,[1] D. J. Suson,[52] H. Tajima,[2]‡ H. Takahashi,[32] T. Takahashi,[39] T. Tanaka,[2]‡ J. B. Thayer,[2] J. G. Thayer,[2] G. Theureau,[22] D. J. Thompson,[18] L. Tibaldo,[8,4,9] O. Tibolla,[53] D. F. Torres,[54,49] G. Tosti,[11,12] A. Tramacere,[2,55] Y. Uchiyama,[2]‡ T. L. Usher,[2] V. Vasileiou,[18,19,20] C. Venter,[18,56] N. Vilchez,[42] V. Vitale,[44,57] A. P. Waite,[2] P. Wang,[2] B. L. Winer,[10] K. S. Wood,[1] R. Yamazaki,[32] T. Ylinen,[36,58,26] M. Ziegler[47]

Recent observations of supernova remnants (SNRs) hint that they accelerate cosmic rays to energies close to ~10^{15} electron volts. However, the nature of the particles that produce the emission remains ambiguous. We report observations of SNR W44 with the Fermi Large Area Telescope at energies between 2×10^8 electron volts and 3×10^{11} electron volts. The detection of a source with a morphology corresponding to the SNR shell implies that the emission is produced by particles accelerated there. The gamma-ray spectrum is well modeled with emission from protons and nuclei. Its steepening above ~10^9 electron volts provides a probe with which to study how particle acceleration responds to environmental effects such as shock propagation in dense clouds and how accelerated particles are released into interstellar space.

Galactic cosmic rays (GCRs) are thought to be accelerated in the expanding shock waves of supernova remnants (SNRs) (*1*, *2*), a conjecture that has been strengthened by recent observations of young SNRs in x-rays (*3*) and TeV gamma rays (*4*–*6*). Magnetic field amplification is essential to make the maximum particle energy attainable large enough to explain the GCRs (*7*). It also implies that a large fraction of the kinetic energy released by a supernova explosion is transferred to cosmic rays (*8*). If strong magnetic fields are present in the gamma-ray–emitting region, the TeV images of young SNRs (*4*–*6*) are more likely to show the accelerated protons and nuclei via their hadronic interactions with the ambient gas and subsequent π^0 decays into gamma rays. However, the identification has been inconclusive because high-energy electrons can also shine in gamma rays via bremsstrahlung and/or inverse Compton processes. Observations in the GeV domain are necessary to disentangle the emission mechanisms by means of spectral differences in this energy band.

Environmental effects can complicate the interpretation of the gamma-ray emission. For instance, enhanced π^0-decay emission can be expected in those SNRs interacting with a molecular cloud (*9*, *10*) because of the higher gas density, which makes the interactions between cosmic-ray nuclei and the gas more frequent. Yet the dense gas slows down the shock and the overall acceleration efficiency, and the acceleration rate can be much reduced because of interactions between the shock and dense gas. Even without strong shell-cloud interactions, the shock is decelerated in the late stage of SNR evolution. Such evolution of particle acceleration (*11*, *12*) can be probed with observations of GeV to TeV gamma rays from SNRs.

Here, we report GeV observations of the middle-aged (~2.0×10^4 years) SNR W44 with the Large Area Telescope (LAT) on board the Fermi Gamma-ray Space Telescope. W44 is known to be interacting with a molecular cloud on the basis of observations of lines of CO (*13*), OH masers (*14*), and near- and mid-infrared (IR) from shocked H_2 (*15*, *16*). In the GeV domain, the EGRET instrument aboard the Compton Gamma Ray Observatory detected a source in the vicinity of the SNR (*17*), although its association with W44 was not clear. The Fermi LAT is a pair-conversion detector capable of measuring gamma rays in the GeV domain (*18*). We analyzed the Fermi LAT data accumulated between 4 August 2008 and 13 July 2009 in the region around W44. Details of event selections for this analysis are summarized in the supporting online material (SOM).

The gamma-ray emission spatially associated with SNR W44 is visible in Fig. 1, well above the GeV emission from the Galactic disc. The source corresponds to 0FGL J1855.9+0126 in the Fermi bright source list (*19*). A detailed analysis reveals that the GeV emission is significantly extended (see SOM) compared with that of a point source case. Therefore, it is difficult to attribute most of the gamma rays to the radio pulsar in W44, PSR B1853+01 (*20*), or its pulsar wind nebula (PWN), which extends only ~1′ to 2′ in x-rays (*21*) and radio (*22*). To extract the gamma-ray morphology of the source, we applied an image deconvolution technique (Fig. 2 and SOM). The resemblance between the gamma-ray and infrared-ring morphologies supports the inference that the bulk of the emission comes from the SNR shell rather than from the unresolved pulsar.

To test the source morphology and determine its spectrum, we performed a maximum likelihood analysis (*23*). The gamma-ray emission model used in the analysis includes individual sources detected in the 11 months, the Galactic diffuse emission (resulting from cosmic-ray interactions with interstellar medium and radiation), and an isotropic component (extragalactic and instrumental backgrounds). For the diffuse backgrounds, we used models released by the LAT collaboration (*23*). In order to quantitatively confirm that the gamma-ray emission is associated with the SNR shell, we compared the likelihood values obtained with the following source shapes:

(i) a point source, (ii) a uniform flux within an ellipse, (iii) a uniform flux within an elliptical ring, and (iv) a uniform elliptical ring plus a point source at the pulsar position (Fig. 2). The single elliptical ring yields the best likelihood and rejects the filled ellipse and point source hypotheses at the >8 σ and >16 σ confidence levels, respectively. The extended ring emission is detected at the 62 σ confidence level above the intense and structured Galactic background in this direction. These results, together with the lack of detection of an additional point source at the pulsar position in case iv, imply that the bulk of the gamma rays comes from the shell, as suggested by the deconvolved image. The 95% upper limit to pulsar and/or PWN flux is 1.6×10^{-7} photons cm^{-2} s^{-1} above 100 MeV. We also searched for gamma-ray pulsation from PSR B1853+01 by using ephemerides provided by the Jodrell Bank and Nançay radio telescopes as in (*24*) but valid through July 2009. However, none was seen (H test < 5).

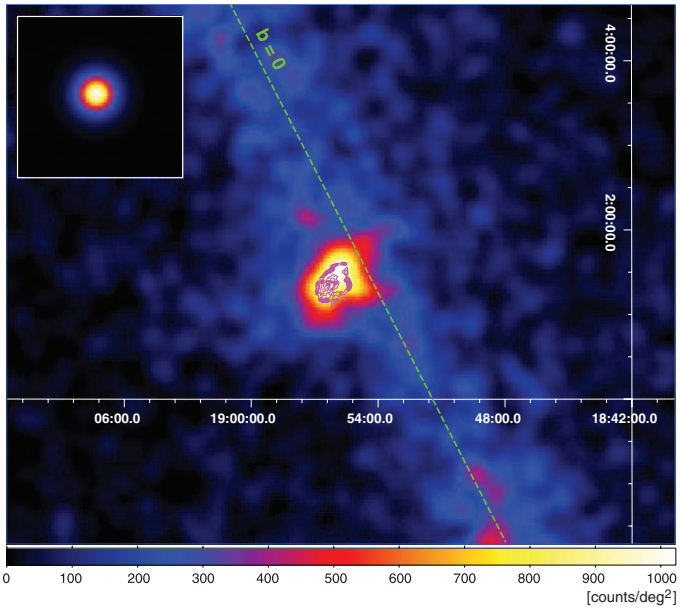

Fig. 1. Fermi LAT image (2 to 10 GeV) of the region where SNR W44 is located. North is up and east is to the left. The color scale indicates count per solid angle on a linear scale. The dotted green line corresponds to the Galactic plane (b = 0°). The radio image of W44 as seen in 20-cm wavelength by the Very Large Array (*31*) is overlaid as the magenta contours. **(Inset)** An image of a simulated point source. In the simulation, spectral parameters of the W44 emission are assumed.

The spectral energy distribution (SED) of the source is seen to steepen toward high energies (Fig. 3). To obtain general characteristics of the spectrum, we fitted it with simple functions. For a broken power law where the photon index is abruptly changed at a break energy, the photon indices are $\Gamma_1 = 2.06 \pm 0.03$ [1σ statistical error (stat)] ± 0.07 [1σ systematic error (sys)] at low energy and $\Gamma_2 = 3.02 \pm 0.10$ (stat) ± 0.12 (sys) at high energy with a break energy of $E_{break} = 1.9 \pm 0.2$ (stat) ± 0.3 (sys) GeV. The likelihood-ratio test between a broken and a single power law disfavors the latter at the significance of 14 σ. The resulting gamma-ray flux integrated above 100 MeV (*25*) amounts to $F_{>100\ MeV} = [1.22 \pm 0.05$ (stat) ± 0.23 (sys)] $\times 10^{-6}$ photons cm^{-2} s^{-1}.

The shell-like morphology and spectral shape of the GeV emission provide information about its origin in the SNR. Most of the emission comes from the SNR shell, which is known to interact with molecular clouds. When high-energy particles interact with dense gas, two emission processes become important: π^0 decays and electron bremsstrahlung. Simple model curves with dominant π^0-decay emission fit the data reasonably well (see SOM for description of the model). In the model, protons and electrons are injected with the constant rate and fixed spectral shape over the age of the SNR (2.0×10^4 years). Although the age should include some uncertainties, the results, particularly in the Fermi LAT energy range, are insensitive to the assumed age. The ratio of injected electrons to protons was fixed at $K_{ep} = 0.01$ to be roughly consistent with

[1]Space Science Division, Naval Research Laboratory, Washington, DC 20375, USA. [2]W. W. Hansen Experimental Physics Laboratory, Kavli Institute for Particle Astrophysics and Cosmology, Department of Physics and SLAC National Accelerator Laboratory, Stanford University, Stanford, CA 94305, USA. [3]Istituto Nazionale di Fisica Nucleare (INFN), Sezione di Pisa, I–56127 Pisa, Italy. [4]Laboratoire Astrophysique Instrumentation Modélisation, Commissariat à l'Énergie Atomique (CEA)–Institut de Recherche sur les Lois Fondamentales de l'Univers (IRFU)/CNRS/Université Paris Diderot, Service d'Astrophysique, CEA Saclay, 91191 Gif sur Yvette, France. [5]Istituto Nazionale di Fisica Nucleare, Sezione di Trieste, I–34127 Trieste, Italy. [6]Dipartimento di Fisica, Università di Trieste, I–34127 Trieste, Italy. [7]Rice University, Department of Physics and Astronomy, MS–108, Post Office Box 1892, Houston, TX 77251, USA. [8]Istituto Nazionale di Fisica Nucleare, Sezione di Padova, I–35131 Padova, Italy. [9]Dipartimento di Fisica "G. Galilei," Università di Padova, I–35131 Padova, Italy. [10]Department of Physics, Center for Cosmology and Astro-Particle Physics, The Ohio State University, Columbus, OH 43210, USA. [11]Istituto Nazionale di Fisica Nucleare, Sezione di Perugia, I–06123 Perugia, Italy. [12]Dipartimento di Fisica, Università degli Studi di Perugia, I–06123 Perugia, Italy. [13]Dipartimento di Fisica "M. Merlin" dell'Università e del Politecnico di Bari, I–70126 Bari, Italy. [14]Istituto Nazionale di Fisica Nucleare, Sezione di Bari, 70126 Bari, Italy. [15]Laboratoire Leprince-Ringuet, École Polytechnique, CNRS/Institut National de Physique Nucléaire et de Physique des Particules (IN2P3), Palaiseau, France. [16]Department of Physics, University of Washington, Seattle, WA 98195–1560, USA. [17]Istituto di Astrofisica Spaziale e Fisica Cosmica, Istituto Nazionale di Astrofisica (INAF), I–20133 Milano, Italy. [18]NASA Goddard Space Flight Center, Greenbelt, MD 20771, USA. [19]Center for Research and Exploration in Space Science and Technology (CRESST), NASA Goddard Space Flight Center, Greenbelt, MD 20771, USA. [20]University of Maryland, Baltimore County, Baltimore, MD 21250, USA. [21]George Mason University, Fairfax, VA 22030, USA. [22]Laboratoire de Physique et Chemie de l'Environnement (LPCE), LPCE UMR 6115 CNRS, F–45071 Orléans Cedex 02, France, and Station de Radioastronomie de Nançay, Observatoire de Paris, CNRS/Institut National des Sciences de l'Univers (INSU), F–18330 Nançay, France. [23]Laboratoire de Physique Théorique et Astroparticules, Université Montpellier 2, CNRS/IN2P3, Montpellier, France. [24]Department of Physics and Astronomy, Sonoma State University, Rohnert Park, CA 94928–3609, USA. [25]Department of Physics, Stockholm University, AlbaNova, SE–106 91 Stockholm, Sweden. [26]The Oskar Klein Centre for Cosmoparticle Physics, AlbaNova, SE–106 91 Stockholm, Sweden. [27]Agenzia Spaziale Italiana (ASI) Science Data Center, I–00044 Frascati (Roma), Italy. [28]Dipartimento di Fisica, Università di Udine and Istituto Nazionale di Fisica Nucleare, Sezione di Trieste, Gruppo Collegato di Udine, I–33100 Udine, Italy. [29]Centre d'Études Nucléaires Bordeaux Gradignan, Université de Bordeaux, UMR 5797, 33175 Gradignan, France. [30]Centre d'Études Nucléaires Bordeaux Gradignan, CNRS/IN2P3, UMR 5797, Gradignan 33175, France. [31]Jodrell Bank Centre for Astrophysics, School of Physics and Astronomy, The University of Manchester, Manchester M13 9PL, UK. [32]Department of Physical Sciences, Hiroshima University, Higashi-Hiroshima, Hiroshima 739–8526, Japan. [33]University of Maryland, College Park, MD 20742, USA. [34]Istituto Nazionale di Fisica Nucleare, Sezione di Trieste, and Università di Trieste, I–34127 Trieste, Italy. [35]University of Alabama in Huntsville, Huntsville, AL 35899, USA. [36]Department of Physics, Royal Institute of Technology (KTH), AlbaNova, SE–106 91 Stockholm, Sweden. [37]Department of Physics, Tokyo Institute of Technology, Meguro City, Tokyo 152–8551, Japan. [38]Waseda University, 1-104 Totsukamachi, Shinjuku-ku, Tokyo 169–8050, Japan. [39]Institute of Space and Astronautical Science, Japan Aerospace Exploration Agency (JAXA), 3-1-1 Yoshinodai, Sagamihara, Kanagawa 229–8510, Japan. [40]Department of Physics, Graduate School of Science, University of Tokyo, 7-3-1 Hongo, Bunkyo-ku, Tokyo 113–0033, Japan. [41]Cosmic Radiation Laboratory, Institute of Physical and Chemical Research (RIKEN), Wako, Saitama 351–0198, Japan. [42]Centre d'Étude Spatiale des Rayonnements, CNRS/Université Paul Sabatier (UPS), BP 44346, F–30128 Toulouse Cedex 4, France. [43]Max-Planck-Institut für Radioastronomie, Auf dem Hügel 69, 53121 Bonn, Germany. [44]Istituto Nazionale di Fisica Nucleare, Sezione di Roma "Tor Vergata," I–00133 Roma, Italy. [45]Department of Physics and Astronomy, University of Denver, Denver, CO 80208, USA. [46]Max-Planck Institut für Extraterrestrische Physik, 85748 Garching, Germany. [47]Santa Cruz Institute for Particle Physics, Department of Physics and Department of Astronomy and Astrophysics, University of California at Santa Cruz, Santa Cruz, CA 95064, USA. [48]Institut für Astro- und Teilchenphysik and Institut für Theoretische Physik, Leopold-Franzens-Universität Innsbruck, A–6020 Innsbruck, Austria. [49]Institut de Ciencies de l'Espai (IEEC-CSIC), Campus UAB, 08193 Barcelona, Spain. [50]Space Sciences Division, NASA Ames Research Center, Moffett Field, CA 94035–1000, USA. [51]NYCB Real-Time Computing Incorporated, Lattingtown, NY 11560–1025, USA. [52]Department of Chemistry and Physics, Purdue University Calumet, Hammond, IN 46323–2094, USA. [53]Max-Planck-Institut für Kernphysik, D–69029 Heidelberg, Germany. [54]Institució Catalana de Recerca i Estudis Avançats (ICREA), 08010 Barcelona, Spain. [55]Consorzio Interuniversitario per la Fisica Spaziale (CIFS), I–10133 Torino, Italy. [56]North-West University, Potchefstroom Campus, Potchefstroom 2520, South Africa. [57]Dipartimento di Fisica, Università di Roma "Tor Vergata," I–00133 Roma, Italy. [58]School of Pure and Applied Natural Sciences, University of Kalmar, SE–391 82 Kalmar, Sweden.

*National Research Council Research Associate, National Academy of Sciences, Washington, DC 20001, USA.
†Royal Swedish Academy of Sciences Research Fellow.
‡To whom correspondence should be addressed. E-mail: ttanaka@slac.stanford.edu (T.T.); uchiyama@slac.stanford.edu (Y.U.); htajima@slac.stanford.edu (H.T.)

the cosmic-ray composition observed at Earth, where K_{ep} is defined as a ratio of particle numbers at $p = 1$ GeV/c. The ambient gas density was assumed to be $n = 100$ cm^{-3}, which is the estimated averaged density in the molecular cloud interacting with W44 (*15*). Both proton and electron spectra have a spectral break at $p_{br} = 9$ GeV/c. The power-law indices are $s_1 = 1.74$ below the break, whereas the indices are $s_2 = 3.7$ above the break. The spectral indices below the break were chosen to explain the observed radio synchrotron spectrum with $\alpha = \Gamma - 1 = 0.37$ (*26*). In this model, the total kinetic energy of protons and electrons integrated above 100 MeV amount to $W_p = 6 \times 10^{49}$ erg and $W_e = 1 \times 10^{48}$ erg. The spectral index of $s_1 = 1.73$ deduced from the radio index is harder compared with $s_1 = 2.0$ expected from the standard acceleration theory. The flat radio spectrum might be due to processes such as reacceleration of preexisting cosmic-ray electrons (*27*). In such cases, spectral index of protons could be different from that of electrons. Assuming the standard value of $s_1 = 2.0$ yields $s_2 = 3.3$ and $p_{br} = 7$ GeV/c for protons.

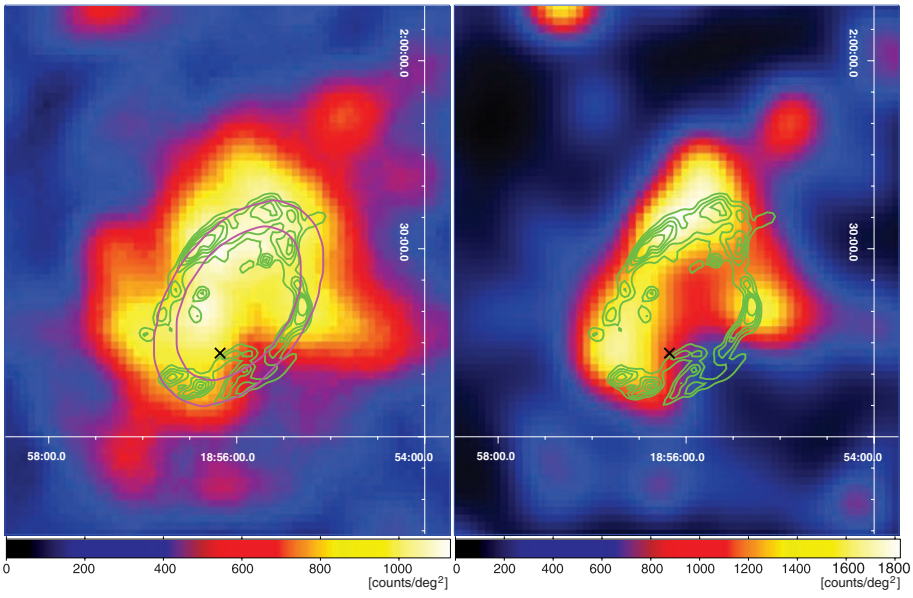

Fig. 2. Close-up images (2 to 10 GeV) of the SNR W44 region obtained with Fermi LAT. (**Left**) Count map. (**Right**) Deconvolved image that should be used to see the large-scale structure of the source, not to discern small structures with angular scales of <10′, which can be affected by statistical fluctuations. Such features should therefore not be taken as indicative of the true source morphology. The black cross on each image indicates the location of a radio pulsar, PSR B1853+01, which is believed to be associated with SNR W44 because its estimated distance of 3 kpc and characteristic age of 2×10^4 years are consistent with those independently obtained for the SNR (*20*). The green contours represent the 4.5-μm IR image by the Spitzer Space Telescope Infrared Array Camera (*16*), which traces shocked H_2. The magenta ellipses in the left image describe the spatial models used for the maximum likelihood analysis. Uniform emission inside the outer ellipse and uniform emission in the region between the inner and outer ellipses were among the models considered for the spatial distribution.

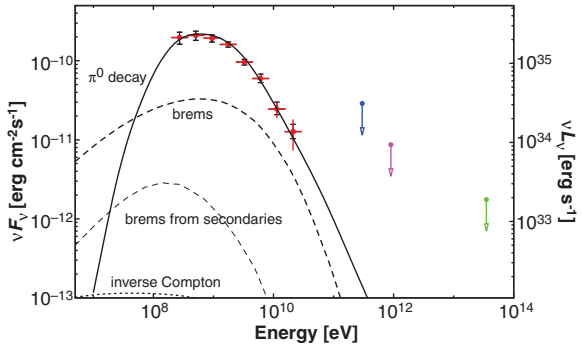

Fig. 3. Fermi LAT spectral energy distributions (SEDs) of SNR W44. The gamma-ray flux of each point was obtained by binning the gamma-ray data in a range of 0.2 to 30 GeV into eight energy intervals and performing a binned likelihood analysis on each energy bin. The source shape is assumed to be the elliptical ring shown in Fig. 2. The vertical red lines and the black caps represent 1 σ statistical errors and systematic errors, respectively. The SED is insensitive to the choice of reasonable diffuse background models within the ~10% level. It is also insensitive to the choice of the gamma-ray source shape between the elliptical ring and filled ellipse. Each curve corresponds to contributions from each emission process: π^0 decay (solid), electron bremsstrahlung (dashed), inverse Compton scattering (dots), and bremsstrahlung from secondary electrons and positrons, which are decay products of $\pi^\pm$ produced by the same hadronic interactions as π^0 production (thin dashed) for a simple model in which most of the emission detected by the Fermi LAT is attributed to π^0 decays. The spectra of protons and electrons have a form of $\propto p^{-s_1}(1 + p/p_{br})^{s_1 - s_2}$. A magnetic field of $B = 70$ μG is given from the radio flux, which is not shown here. In addition to the Fermi LAT data, currently available upper limits in the TeV energies by Whipple (*32*) (blue), High Energy Gamma Ray Astronomy (HEGRA) (*33*) (magenta), and Milagro (*34*) (green) are plotted. Because the Whipple and HEGRA upper limits are given in flux integrated above their threshold energies, we converted them to energy flux assuming power-law spectra with photon indices of 3.0.

Instead, if one attempts to attribute the bulk of the gamma-ray flux to electron bremsstrahlung, the break in the Fermi LAT spectrum requires a break in the parent electron spectrum. In order to explain the power-law radio spectrum up to 10 GHz (*26*) at the same time, a strong magnetic field more intense than ~100 μG is necessary to have the corresponding break in the synchrotron spectrum at a frequency higher than 10 GHz. In this case, a high ambient density greater than ~1000 cm^{-3} is needed to explain the Fermi LAT flux (see SOM for modeling details). A strong magnetic field and high gas density are plausible if the observed emission is radiated mostly from the region where the shell is interacting with dense gas (*15*). However, electron bremsstrahlung can dominate over π^0-decay emission in the GeV band only with $K_{ep} > 0.1$, far greater than the observed cosmic-ray composition ratio near Earth.

Although not necessarily relevant to the shell-cloud interaction, another emission process, inverse Compton scattering of electrons, can in principle produce gamma rays at GeV energies. In the model shown in Fig. 3, the calculated gamma-ray flux from inverse Compton scattering is ~1×10^{-13} erg cm^{-2} s^{-1} at ~100 MeV to 1 GeV when the interstellar radiation field (*28*) at the location of W44 is assumed as target photons for electrons. The interstellar radiation field includes optical radiation from stars with the energy density of 0.96 eV cm^{-3} and infrared radiation with 0.93 eV cm^{-3} in addition to the cosmic microwave background at 0.26 eV cm^{-3}. In order for the inverse Compton emission to be enhanced to the flux level of the Fermi LAT spectrum, total energy in electrons is required to be as large as ~10^{51} erg, or the local soft photon field should be denser at least by one order of magnitude than the interstellar radiation field to reduce the total electron energy to <10^{50} erg. SNR W44 itself is an infrared radiation source and can provide additional target photons for the inverse Compton process. However, estimated energy density of infrared photons from W44 is 0.69 eV cm^{-3} (*29*), which is even lower than that of the interstellar radiation field. Therefore, it is unlikely that the inverse Compton scattering is the dominant emission mechanism in the GeV band. For the same reason, it is difficult to attribute the gamma-ray emission to the PWN, from which inverse Compton radiation is generally expected in the GeV band.

Most plausible is that π^0 decays are responsible for the gamma-ray emission, although the bremsstrahlung scenario cannot be ruled out completely. In order to fit the Fermi LAT spectrum with π^0-decay emission, a spectral break in the proton spectrum is needed at fairly low energy, around 10 GeV/*c*. One possible mechanism to explain the spectral break is that particles escape from their acceleration sites, that is, the SNR shells. Theories predict that very high energy particles above ~TeV can be confined only during the early stage of SNR evolution (*11*, *12*). Because W44 is a middle-aged SNR with estimated age of $\sim 2.0 \times 10^4$ years, most particles accelerated up to higher energies in the past could have escaped from its shell and cannot contribute to the gamma-ray emission we are observing now.

In the case of W44, the effect of particle escape can be enhanced because of the interaction between the shell and the dense, largely neutral molecular gas. Magnetic turbulence, which is required to confine and efficiently accelerate particles, is considered to be substantially damped. Thus, particles can easily escape from the shell at an earlier stage of SNR evolution (*30*) compared with the case where an SNR is expanding in a more rarefied medium. For W44, parts of the shock are expanding into clumps and interclump gas with densities of ~10 to ~100 cm^{-3} (*15*). The Fermi LAT spectrum indicates that the slow shock velocity (<500 km s^{-1}) and efficient damping can limit the maximum particle energy to a few GeV. Our results for W44 demonstrate the capability of the Fermi LAT for morphological and spectral studies of GeV emission from Galactic SNRs, which allow us to study the escape of energetic particles from SNR shells into interstellar space, the evolution of SNR shocks during the age of the SNR, and the impact of a dense environment.

References and Notes

1. R. Blandford, D. Eichler, *Phys. Rep.* **154**, 1 (1987).
2. M. A. Malkov, L. O'C. Drury, *Rep. Prog. Phys.* **64**, 429 (2001).
3. S. P. Reynolds, *Annu. Rev. Astron. Astrophys.* **46**, 89 (2008).
4. F. A. Aharonian *et al.*, *Nature* **432**, 75 (2004).
5. F. A. Aharonian *et al.*, *Astron. Astrophys.* **464**, 235 (2007).
6. F. A. Aharonian *et al.*, *Astrophys. J.* **661**, 236 (2007).
7. A. R. Bell, S. G. Lucek, *Mon. Not. R. Astron. Soc.* **321**, 433 (2001).
8. E. G. Berezhko, H. J. Völk, *Astron. Astrophys.* **492**, 695 (2008).
9. F. A. Aharonian, L. O'C. Drury, H. J. Völk, *Astron. Astrophys.* **285**, 645 (1994).
10. L. O'C. Drury, F. A. Aharonian, H. J. Völk, *Astron. Astrophys.* **287**, 959 (1994).
11. V. S. Ptuskin, V. N. Zirakashvili, *Astron. Astrophys.* **429**, 755 (2005).
12. S. Gabici, F. A. Aharonian, *Astrophys. J.* **665**, L131 (2007).
13. M. Seta *et al.*, *Astron. J.* **127**, 1098 (2004).
14. I. M. Hoffman, W. M. Goss, C. L. Brogan, M. J. Claussen, *Astrophys. J.* **627**, 803 (2005).
15. W. T. Reach, J. Rho, T. H. Jarrett, *Astrophys. J.* **618**, 297 (2005).
16. W. T. Reach *et al.*, *Astron. J.* **131**, 1479 (2006).
17. J. A. Esposito, S. D. Hunter, G. Kanbach, P. Sreekumar, *Astrophys. J.* **461**, 820 (1996).
18. W. B. Atwood *et al.*, *Astrophys. J.* **697**, 1071 (2009).
19. A. A. Abdo *et al.*, *Astrophys. J.* **183** (suppl.), 46 (2009).
20. A. Wolszczan, J. M. Cordes, R. J. Dewey, *Astrophys. J.* **372**, L99 (1991).
21. R. Petre, K. D. Kuntz, R. L. Shelton, *Astrophys. J.* **579**, 404 (2002).
22. D. A. Frail, E. B. Giacani, W. M. Goss, G. Dubner, *Astrophys. J.* **464**, L165 (1996).
23. Fermi Science Support Center, http://fermi.gsfc.nasa.gov/ssc/.
24. A. A. Abdo *et al.*, The first Fermi Large Area Telescope catalog of gamma-ray pulsars, http://arxiv.org/abs/0910.1608.
25. Although the analysis was performed by using events above 200 MeV, the quoted flux was obtained by extrapolating the best-fit function down to 100 MeV to make it easier to compare the value with past publications on GeV gamma-ray observations.
26. G. Castelletti, G. Dubner, C. Brogan, N. E. Kassim, *Astron. Astrophys.* **471**, 537 (2007).
27. A. M. Bykov, R. A. Chevalier, D. C. Ellison, Y. A. Uvarov, *Astrophys. J.* **538**, 203 (2000).
28. T. A. Porter, I. V. Moskalenko, A. W. Strong, *Astrophys. J.* **648**, L29 (2006).
29. O. C. de Jager, A. Mastichiadis, *Astrophys. J.* **482**, 874 (1997).
30. V. S. Ptuskin, V. N. Zirakashvili, *Astron. Astrophys.* **403**, 1 (2003).
31. D. J. Helfand, R. H. Becker, R. L. White, A. Fallon, S. Tuttle, *Astron. J.* **131**, 2525 (2006).
32. J. H. Buckley *et al.*, *Astron. Astrophys.* **329**, 639 (1998).
33. F. A. Aharonian *et al.*, *Astron. Astrophys.* **395**, 803 (2002).
34. A. A. Abdo *et al.*, *Astrophys. J.* **700**, L127 (2009).

35. The Fermi LAT Collaboration acknowledges support from a number of agencies and institutes for both development and the operation of the LAT as well as scientific data analysis. These include NASA and Department of Energy in the United States; CEA/Irfu, IN2P3/CNRS, and Centre National d'Études Spatiales in France; ASI, INFN, and INAF in Italy; Ministry of Education, Culture, Sports, Science, and Technology, High Energy Accelerator Research Organization (KEK) and JAXA in Japan; and the K. A. Wallenberg Foundation, the Swedish Research Council, and the National Space Board in Sweden.

Supporting Online Material

www.sciencemag.org/cgi/content/full/science.1182787/DC1
Materials and Methods
SOM Text
Figs. S1 and S2
References and Notes

2 October 2009; accepted 29 December 2009
Published online 7 January 2010;
10.1126/science.1182787
Include this information when citing this paper.

Ferroelectric Control of Spin Polarization

V. Garcia,[1] M. Bibes,[1]* L. Bocher,[2] S. Valencia,[3] F. Kronast,[3] A. Crassous,[1] X. Moya,[4] S. Enouz-Vedrenne,[5] A. Gloter,[2] D. Imhoff,[2] C. Deranlot,[1] N. D. Mathur,[4] S. Fusil,[1,6] K. Bouzehouane,[1] A. Barthélémy[1]

A current drawback of spintronics is the large power that is usually required for magnetic writing, in contrast with nanoelectronics, which relies on "zero-current," gate-controlled operations. Efforts have been made to control the spin-relaxation rate, the Curie temperature, or the magnetic anisotropy with a gate voltage, but these effects are usually small and volatile. We used ferroelectric tunnel junctions with ferromagnetic electrodes to demonstrate local, large, and nonvolatile control of carrier spin polarization by electrically switching ferroelectric polarization. Our results represent a giant type of interfacial magnetoelectric coupling and suggest a low-power approach for spin-based information control.

Controlling the spin degree of freedom by purely electrical means is currently an important challenge in spintronics (*1*, *2*). Approaches based on spin-transfer torque (*3*) have proven very successful in controlling the direction of magnetization in a ferromagnetic layer, but they require the injection of high current densities. An ideal solution would rely on the application of an electric field across an insulator, as in existing nanoelectronics. Early experiments have demonstrated the volatile modulation of spin-based properties with a gate voltage applied through a dielectric. Notable examples include the gate control of the spin-orbit interaction in III-V quantum wells (*4*), the Curie temperature T_C (*5*), or the magnetic anisotropy (*6*) in magnetic semiconductors with carrier-mediated exchange interactions; for example, (Ga,Mn)As or (In,Mn)As. Electric field–induced modifications of magnetic anisotropy at room temperature have also been reported recently in ultrathin Fe-based layers (*7*, *8*).

[1]Unité Mixte de Physique CNRS/Thales, 1 Avenue Augustin Fresnel, Campus de l'Ecole Polytechnique, 91767 Palaiseau, France, and Université Paris-Sud, 91405 Orsay, France. [2]Laboratoire de Physique des Solides, Université Paris-Sud, CNRS UMR-8502, 91405 Orsay, France. [3]Helmholtz-Zentrum-Berlin, Berliner Elektronen-Speicherring Gesellschaft für Synchrotronstrahlung (BESSY), Albert-Einstein-Strasse 15,12489 Berlin, Germany. [4]Department of Materials Science, University of Cambridge, Cambridge, CB2 3QZ, UK. [5]Thales Research and Technology, 1 Avenue Augustin Fresnel, Campus de l'Ecole Polytechnique, 91767 Palaiseau, France. [6]Université d'Evry-Val d'Essonne, Boulevard François Mitterrand, 91025 Evry cedex, France.

*To whom correspondence should be addressed. E-mail: manuel.bibes@thalesgroup.com